Frontiers of Information Technology & Electronic Engineering
www.jzus.zju.edu.cn; engineering.cae.cn; www.springerlink.com
ISSN 2095-9184 (print); ISSN 2095-9230 (online)
E-mail: jzus@zju.edu.cn

Time-varying formation tracking for uncertain second-order nonlinear multi-agent systems*

Mao-peng RAN‡, Li-hua XIE, Jun-cheng LI

School of Electrical and Electronic Engineering, Nanyang Technological University, Singapore 639798, Singapore

E-mail: mpran@ntu.edu.sg; ELHXIE@ntu.edu.sg; juncheng001@e.ntu.edu.sg

Received Sept. 12, 2018; Revision accepted Dec. 25, 2018; Crosschecked Jan. 8, 2019

Abstract: Our study is concerned with the time-varying formation tracking problem for second-order multi-agent systems that are subject to unknown nonlinear dynamics and external disturbance, and the states of the followers form a predefined time-varying formation while tracking the state of the leader. The total uncertainty lumps the unknown nonlinear dynamics and the external disturbance, and is regarded as an extended state of the agent. To estimate the total uncertainty, we design an extended state observer (ESO). Then we propose a novel ESO based time-varying formation tracking protocol. It is proved that, under the proposed protocol, the ESO estimation error and the time-varying formation tracking error can be made arbitrarily small. An application to the target enclosing problem for multiple unmanned aerial vehicles (UAVs) verifies the effectiveness and superiority of the proposed approach.

Key words: Multi-agent system; Time-varying formation; Formation tracking; Nonlinear dynamics; Extended state observer (ESO)

https://doi.org/10.1631/FITEE.1800557 **CLC number:** TP13

1 Introduction

There has been a spurt of interest over several decades in the area of formation control of multi-agent systems (Oh et al., 2015; Li and Xie, 2018). It is partly due to the fact that the formation control can find broad application in many engineering fields, such as attitude control of spacecrafts (Du et al., 2016), flying control of unmanned aerial vehicles (UAVs) (Zhu et al., 2017), control of autonomous underwater vehicles (AUVs) (Leonard et al., 2010), and formation control of mobile robots (Li et al., 2017). To improve the intelligence, reliability, and efficiency of multi-agent systems without human intervention, different formation control approaches have been proposed. These approaches can be roughly categorized as the leader-follower strategy, the behavioral approach, the virtual structure method, and the artificial potential mechanism (Liu and Jia, 2012; Peng et al., 2013; Yang et al., 2014). Ren (2007) proposed a consensus based formation control approach to second-order multi-agent systems, and it was shown that the leader-follower strategy, the behavioral approach, and the virtual structure method can be unified in the framework of consensus based approaches. More consensus based formation control approaches can be found in Ren and Sorensen (2008), Guo et al. (2010), Lin et al. (2013), Oh and Ahn (2014), and Dong et al. (2015).

In some practical applications, to accomplish more complex tasks, it is only the first step for a multi-agent system to form a desired time-varying formation. For example, to perform a source seeking or target enclosing task, the whole formation

‡ Corresponding author

* Project supported by the Delta-NTU Corporate Lab through the NRF Corporate Lab@University Scheme

needs to further track the leader's trajectory. In such circumstances, the time-varying formation tracking problem arises; namely, the followers form the predefined time-varying formation when tracking the leader's trajectory. Although there are many different approaches to formation control of multi-agent systems, only a few studies are concerned with the time-varying formation tracking problem. Ren and Sorensen (2008) considered the formation tracking problem for first-order multi-agent systems with a virtual leader. Guo et al. (2010) studied the target enclosing problem for first-order multi-agent systems subject to switching topologies, which is considered as a special case of the formation tracking problem. Lin et al. (2013) adopted a complex Laplacian based formation tracking approach to second-order multi-agent systems. Dong et al. (2017a) studied the time-varying formation tracking problem for second-order multi-agent systems with a leader. Dong et al. (2017b) established the switching topologies counterpart of the approach in Dong et al. (2017a).

In the aforementioned studies on formation control of multi-agent systems (Ren and Sorensen, 2008; Guo et al., 2010; Lin et al., 2013; Oh and Ahn, 2014; Dong et al., 2015, 2017a,b), the dynamics of each agent are limited to be linear. However, most of practical control systems are inherently nonlinear (Khalil, 2002). Therefore, it is meaningful and important to study formation control problems for multi-agent systems with nonlinear dynamics (Meng et al., 2014; Li et al., 2017). What is more, in practice, it is generally hard to establish the accurate mathematical model of the nonlinear dynamics (Bechlioulis and Rovithakis, 2017). To the best of our knowledge, time-varying formation tracking for multi-agent systems subject to unknown nonlinear dynamics is still open. In practical applications, external disturbance may disturb the dynamics of the agents. For example, for an underwater vehicle, the external ocean disturbance, perhaps induced by wave, ocean-current, and so on, cannot be ignored in the control design (Cui et al., 2010; Chen YY et al., 2017b).

In this study, we investigate the time-varying formation tracking problem for multi-agent systems subject to unknown nonlinear dynamics and external disturbance. We model the followers by second-order uncertain nonlinear systems with external disturbance. Our study is inspired by Han (2009), where an active disturbance rejection control (ADRC) approach was proposed. In recent years, ADRC has received increasing attention, in both academia (Guo and Zhao, 2011; Zheng et al., 2012; Jiang et al., 2015; Ran et al., 2017a,b; Hu et al., 2018) and industry (Castañeda et al., 2015; Chang et al., 2015; Herbst, 2016; Lotfi et al., 2016; Wang et al., 2016). In ADRC, the total uncertainties are regarded as an extended state of the system, estimated by an extend state observer (ESO), and finally cancelled out in the control loop. Such design philosophy will be applied to the current study to solve the time-varying formation tracking problem for multi-agent systems with unknown nonlinear dynamics and external disturbance. We design a third-order ESO to estimate the defined extended state, which is the combination of the unknown nonlinear dynamics and external disturbance, and propose a novel ESO based time-varying formation tracking protocol. Rigorous theoretical analysis shows that, under the proposed protocol, the convergence of the ESO estimation error and the time-varying formation tracking error can be guaranteed.

Compared with existing studies, our contributions of are twofold. First, we attempt to tackle the time-varying formation tracking problem for multi-agent systems subject to unknown nonlinear dynamics and external disturbance. In practical applications, the inevitable unknown nonlinear dynamics and external disturbance may reduce the formation performance and even lead to instability of multi-agent systems. In Ren and Sorensen (2008), Guo et al. (2010), Lin et al. (2013), Oh and Ahn (2014), and Dong et al. (2015, 2017a,b), these approaches cannot be applied to deal with the time-varying formation tracking problem related to our study. Second, we propose a novel ESO based time-varying formation tracking protocol. In Guo and Zhao (2011), Zheng et al. (2012), Castañeda et al. (2015), Chang et al. (2015), Jiang et al. (2015), Herbst (2016), Lotfi et al. (2016), Wang et al. (2016), Ran et al. (2017a,b), and Hu et al. (2018), the observer and the control law were both designed in a centralized manner. In this study, we assume that each agent operates solely on the basis of its neighborhood information, and consequently the centralized approaches in Guo and Zhao (2011), Zheng et al. (2012), Castañeda et al. (2015), Chang et al. (2015), Jiang et al. (2015), Herbst (2016), Lotfi et al. (2016), Wang et al. (2016), and Ran et al. (2017a,b), cannot be straightforwardly applied in the considered formation control problem.

2 Preliminaries and problem description

2.1 Notations

$\mathbb{R}$ and $\mathbb{C}$ denote the set of the real numbers and the set of the complex numbers, respectively. $\mathbb{R}^n$ and $\mathbb{R}^{n\times n}$ denote the n-dimensional real vector space and $n\times n$ real matrix space, respectively. $\boldsymbol{X}^{\mathrm{T}}$ represents the transpose of vector or matrix $\boldsymbol{X}$. For $\lambda\in\mathbb{C}$, $\mathrm{Re}(\lambda)$ is the real part of λ. $\|\cdot\|$ represents the Euclidean norm. $\lambda_{\max}(\boldsymbol{P})$ and $\lambda_{\min}(\boldsymbol{P})$ denote the maximum and minimum eigenvalues of matrix $\boldsymbol{P}$, respectively. $\boldsymbol{1}_N\in\mathbb{R}^N$ with one in its elements. $\boldsymbol{I}_N$ denotes the $N\times N$ dimensional identity matrix. $\boldsymbol{A}\otimes\boldsymbol{B}$ denotes the Kronecker product of matrices $\boldsymbol{A}$ and $\boldsymbol{B}$.

2.2 Graph theory

Let a multi-agent system consist of N agents. A directed graph $G=(V,E)$ is used to model the communication among the agents, where $V=\{v_1,v_2,\ldots,v_N\}$ and $E\subseteq V^2$ denote the set of vertices and the set of edges, respectively. The graph is assumed to be simple, i.e., $(v_i,v_i)\notin E$. The adjacency matrix associated with graph G is denoted by $\boldsymbol{A}=[a_{ij}]\in\mathbb{R}^{N\times N}$ with $a_{ij}\in\{0,1\}$, $i,j=1,2,\ldots,N$. $a_{ij}=1$ means that agent i can obtain information from agent j (namely, $(v_i,v_j)\in E$), while $a_{ij}=0$ means that there is no information flow from agent j to agent i (namely, $(v_i,v_j)\notin E$). The neighborhood of a vertex v_i is denoted by $N_i=\{v_j|(v_i,v_j)\in E\}$, and the degree matrix is defined as $\boldsymbol{D}=\mathrm{diag}[d_i]\in\mathbb{R}^{N\times N}$ with $d_i=\sum_{j\in N_i}a_{ij}$. The Laplacian matrix with graph G is denoted by $\boldsymbol{L}=\boldsymbol{D}-\boldsymbol{A}\in\mathbb{R}^{N\times N}$. A directed path in G is a finite sequence v_{i_1}, v_{i_2}, …, v_{i_l} of vertices such that $(v_{i_j},v_{i_{j+1}})\in E$ for $j=1,2,\ldots,l-1$. An agent is called a leader if it has no neighbor and is called a follower if it has at least one neighbor.

2.3 Problem description

Consider that a multi-agent system consists of $N-1$ followers, labeled from 1 to $N-1$, and one leader, labeled N. $F=\{1,2,\ldots,N-1\}$ is the follower subscript set. The dynamics of follower i ($i\in F$) are given by

$$\begin{cases}\dot{\boldsymbol{x}}_i(t)=\boldsymbol{v}_i(t),\\ \dot{\boldsymbol{v}}_i(t)=f_i(\boldsymbol{x}_i(t),\boldsymbol{v}_i(t))+\boldsymbol{d}_i(t)+\boldsymbol{u}_i(t),\\ \boldsymbol{y}_i(t)=\boldsymbol{x}_i(t),\end{cases}\tag{1}$$

where $\boldsymbol{x}_i(t)\in\mathbb{R}^n$, $\boldsymbol{v}_i(t)\in\mathbb{R}^n$, $\boldsymbol{u}_i(t)\in\mathbb{R}^n$, and $\boldsymbol{y}_i(t)\in\mathbb{R}^n$ are the position, velocity, control input, and measured output vectors of follower i, respectively, $\boldsymbol{d}_i(t)\in\mathbb{R}^n$ is the external disturbance, and $f_i(\cdot):\mathbb{R}^n\times\mathbb{R}^n\to\mathbb{R}^n$ is the unknown continuously differentiable system function. Similar to Dong et al. (2017a,b), the dynamics of the leader are given by

$$\begin{cases}\dot{\boldsymbol{x}}_N(t)=\boldsymbol{v}_N(t),\\ \dot{\boldsymbol{v}}_N(t)=\alpha_{\boldsymbol{x}}\boldsymbol{x}_N(t)+\alpha_{\boldsymbol{v}}\boldsymbol{v}_N(t),\end{cases}\tag{2}$$

where $\boldsymbol{x}_N(t)\in\mathbb{R}^n$ and $\boldsymbol{v}_N(t)\in\mathbb{R}^n$ are the position and velocity vectors of the leader, respectively, and $\alpha_{\boldsymbol{x}}\in\mathbb{R}$ and $\alpha_{\boldsymbol{v}}\in\mathbb{R}$ are known damping constants. Without loss of generality, we assume $n=1$ henceforth.

Remark 1 From Eq. (1), the followers are subject to unknown nonlinear function $f_i(x_i(t),v_i(t))$ and external disturbance $d_i(t)$. If $f_i(x_i(t),v_i(t))\equiv 0$ and $d_i(t)\equiv 0$, the dynamics of each follower become the well-studied double integrator; if $f_i(x_i(t),v_i(t))\equiv 0$, the dynamics of each follower are reduced to the double integrator with external disturbance studied in Galzi and Shtessel (2006); if $f_i(x_i(t),v_i(t))=\alpha_x x_i(t)+\alpha_v v_i(t)$ and $d_i(t)\equiv 0$, the dynamics of each follower become the linear time-invariant second-order system considered in Dong et al. (2017a,b). In Chen YY et al. (2017a,b), the robust formation tracking problem was considered for second-order uncertain nonlinear multi-agent systems. However, in Chen YY et al. (2017a,b), the uncertain nonlinear functions were composed of known base vectors and unknown coefficients, and the velocity vector was assumed to be available directly. In this study, the nonlinear functions $f_i(\cdot)$, $i\in F$, are totally unknown, and the velocity vector of each follower is not available for control design.

Let the time-varying formation for the followers to form be specified as $\boldsymbol{h}_F(t)=[\boldsymbol{h}_1^{\mathrm{T}}(t),\ \boldsymbol{h}_2^{\mathrm{T}}(t),\ \ldots,\ \boldsymbol{h}_{N-1}^{\mathrm{T}}(t)]^{\mathrm{T}}$, where $\boldsymbol{h}_i(t)=[h_{ix}(t),h_{iv}(t)]^{\mathrm{T}}$ ($i\in F$) and $h_{iv}(t)=\dot{h}_{ix}(t)$. Denote $\boldsymbol{\phi}_i(t)=[x_i(t),v_i(t)]^{\mathrm{T}}$, $i=1,2,\ldots,N$.

Definition 1 (Dong et al., 2017a,b) The multi-agent system formed by Eqs. (1) and (2) is said to achieve time-varying formation tracking if for any given bounded initial states,

$$\lim_{t\to\infty} (\boldsymbol{\phi}_i(t) - \boldsymbol{h}_i(t) - \boldsymbol{\phi}_N(t)) = \mathbf{0}_{2\times 1},\ i \in F. \quad (3)$$

Remark 2 As pointed out in Dong et al. (2017a,b), the target enclosing problem and the consensus tracking problem can be regarded as special cases of the time-varying formation tracking problem specified by Definition 1. Specifically, if $\lim_{t\to\infty} \sum_{i=1}^{N-1} \boldsymbol{h}_i(t) = \mathbf{0}_{2\times 1}$, from Eq. (3), we can obtain

$$\lim_{t\to\infty} \sum_{i=1}^{N-1} \boldsymbol{\phi}_i(t) = (N-1) \lim_{t\to\infty} \boldsymbol{\phi}_N(t),$$

which indicates that the leader lies in the center when the time-varying formation tracking is accomplished. Hence, Definition 1 is reduced to the target enclosing problem in the case $\lim_{t\to\infty} \sum_{i=1}^{N-1} \boldsymbol{h}_i(t) = \mathbf{0}_{2\times 1}$. What is more, if $\boldsymbol{h}_F(t) \equiv \mathbf{0}$, Definition 1 becomes the consensus tracking problem.

Then, in this study, we will design the protocol $u_i(t)$, $i \in F$, such that the uncertain nonlinear multi-agent system formed by Eqs. (1) and (2) achieves the time-varying formation tracking specified by Definition 1. To accomplish the purpose, we make the following assumptions:

Assumption 1 The external disturbance $d_i(t)$, $i \in F$, and its derivative $\dot{d}_i(t)$ are uniformly bounded with respect to t.

Assumption 2 There exists at least one directed path from the leader to each follower.

Considering the leader-follower topology structure, the Laplacian matrix $\boldsymbol{L}$ satisfies

$$\boldsymbol{L} = \begin{bmatrix} \boldsymbol{L}_1 & \boldsymbol{L}_2 \\ \mathbf{0}_{1\times(N-1)} & \mathbf{0}_{1\times 1} \end{bmatrix} \in \mathbb{R}^{N\times N}, \quad (4)$$

where $\boldsymbol{L}_1 \in \mathbb{R}^{(N-1)\times(N-1)}$ and $\boldsymbol{L}_2 \in \mathbb{R}^{(N-1)\times 1}$. If Assumption 2 is satisfied, the following lemma holds:

Lemma 1 (Meng et al., 2010) If the directed interaction topology G satisfies Assumption 1, then all the eigenvalues of $\boldsymbol{L}_1$ have positive real parts. What is more, each row sum of $-\boldsymbol{L}_1^{-1}\boldsymbol{L}_2$ is one, and each entry of $-\boldsymbol{L}_1^{-1}\boldsymbol{L}_2$ is nonnegative.

Assumption 3 The state of the leader $\boldsymbol{\phi}_N(t)$, the formation vector $\boldsymbol{h}_i(t)$, $i \in F$, and $\dot{h}_{iv}(t)$ are uniformly bounded with respect to t.

Remark 3 Assumption 3 implies that the leader's state $\boldsymbol{\phi}_N(t)$, the formation vector $\boldsymbol{h}_i(t)$, $i \in F$, and $\dot{h}_{iv}(t)$ are upper-bounded by some constants (which could be large though). The leader's state being bound is reasonable because usually in real applications the leader will not diverge, and similar assumptions can be found in many previous multi-agent studies (Zhang and Lewis, 2012; Lü et al., 2016). Considering that the states of the practical dynamic system are bounded and continuous, and that the control is also bounded due to the inherent actuator limitations, it is impossible and impractical for the states of the followers to form the time-varying formation described by $\boldsymbol{h}_i(t)$ with $[h_{ix}(t), h_{iv}(t), \dot{h}_{iv}(t)]^{\mathrm{T}}$ trending to infinity. Thus, the boundedness requirement of $\boldsymbol{h}_i(t)$ and $\dot{h}_{iv}(t)$ is also reasonable.

3 Main results

In this section, we investigate the time-varying formation tracking protocol design and analysis problems for the multi-agent system formed by Eqs. (1) and (2). We design an ESO to estimate the unmeasurable states and uncertainty, and then present a novel ESO based time-varying formation tracking protocol.

3.1 Time-varying formation tracking protocol design

For follower i ($i \in F$), the extended state is defined as the combination of the unknown nonlinear function $f_i(x_i(t), v_i(t))$ and the external disturbance $d_i(t)$, that is,

$$\xi_i(t) = f_i(x_i(t), v_i(t)) + d_i(t). \quad (5)$$

Then, the following ESO is designed for follower i ($i \in F$):

$$\begin{cases} \dot{\hat{x}}_i(t) = \hat{v}_i(t) + \frac{l_1}{\varepsilon}(x_i(t) - \hat{x}_i(t)), \\ \dot{\hat{v}}_i(t) = \hat{\xi}_i(t) + \frac{l_2}{\varepsilon^2}(x_i(t) - \hat{x}_i(t)) + u_i(t), \\ \dot{\hat{\xi}}_i(t) = \frac{l_3}{\varepsilon^3}(x_i(t) - \hat{x}_i(t)), \end{cases} \quad (6)$$

where $[\hat{x}_i(t), \hat{v}_i(t), \hat{\xi}_i(t)]^{\mathrm{T}} \in \mathbb{R}^3$ is the observer state, ε is a small positive constant, and $[l_1, l_2, l_3]^{\mathrm{T}} \in \mathbb{R}^3$ is the selected observer gain, so that the following matrix is Hurwitz:

$$\boldsymbol{E} = \begin{bmatrix} -l_1 & 1 & 0 \\ -l_2 & 0 & 1 \\ -l_3 & 0 & 0 \end{bmatrix} \in \mathbb{R}^{3\times 3}. \quad (7)$$

The scaled ESO estimation error is defined as $\boldsymbol{\eta}_i(t) = [\eta_{i1}(t), \eta_{i2}(t), \eta_{i3}(t)]^{\rm T} \in \mathbb{R}^3$, $i \in F$, with

$$\begin{cases} \eta_{i1}(t) = \frac{1}{\varepsilon^2}(x_i(t) - \hat{x}_i(t)), \\ \eta_{i2}(t) = \frac{1}{\varepsilon}(v_i(t) - \hat{v}_i(t)), \\ \eta_{i3}(t) = \xi_i(t) - \hat{\xi}_i(t). \end{cases} \tag{8}$$

Then, from Eqs. (1) and (6), the dynamics of $\boldsymbol{\eta}_i(t)$, $i \in F$, can be written as

$$\begin{cases} \varepsilon\dot{\eta}_{i1}(t) = \eta_{i2}(t) - l_1\eta_{i1}(t), \\ \varepsilon\dot{\eta}_{i2}(t) = \eta_{i3}(t) - l_2\eta_{i1}(t), \\ \varepsilon\dot{\eta}_{i3}(t) = \varepsilon\dot{\xi}_i(t) - l_3\eta_{i1}(t). \end{cases} \tag{9}$$

Denote $\hat{\boldsymbol{\phi}}_i(t) = [\hat{x}_i(t), \hat{v}_i(t)]^{\rm T}$, $i \in F$. Let the eigenvalues of $\boldsymbol{L}_1$ be λ_i, $i \in F$, with $0 < {\rm Re}(\lambda_1) \le {\rm Re}(\lambda_2) \le \ldots \le {\rm Re}(\lambda_{N-1})$. The ESO based time-varying formation tracking protocol is given by

$$\begin{aligned} u_i(t) =& \boldsymbol{K} \sum_{j\in N_i, j\neq N} a_{ij} \Big((\hat{\boldsymbol{\phi}}_i(t) - \boldsymbol{h}_i(t)) \\ & - (\hat{\boldsymbol{\phi}}_j(t) - \boldsymbol{h}_j(t)) \Big) \\ & + \boldsymbol{K} a_{iN} \Big((\hat{\boldsymbol{\phi}}_i(t) - \boldsymbol{h}_i(t)) - \boldsymbol{\phi}_N(t) \Big) \\ & + \boldsymbol{\alpha} \Big(\hat{\boldsymbol{\phi}}_i(t) - \boldsymbol{h}_i(t) \Big) + \dot{h}_{iv}(t) - \hat{\xi}_i(t), \ i \in F, \end{aligned} \tag{10}$$

where

$$\boldsymbol{\alpha} = [\alpha_x, \alpha_v], \boldsymbol{K} = -\delta[{\rm Re}(\lambda_1)]^{-1} R^{-1} \boldsymbol{B}_2^{\rm T} \boldsymbol{P}_{\boldsymbol{K}}.$$

Here $\delta > 0.5$, and $\boldsymbol{P}_{\boldsymbol{K}} \in \mathbb{R}^{2\times 2}$ is the solution of the following equation:

$$\begin{aligned} \boldsymbol{P}_{\boldsymbol{K}} \left(\boldsymbol{B}_1\boldsymbol{B}_2^{\rm T} + \boldsymbol{B}_2\boldsymbol{\alpha} \right) + \left(\boldsymbol{B}_1\boldsymbol{B}_2^{\rm T} + \boldsymbol{B}_2\boldsymbol{\alpha} \right)^{\rm T} \boldsymbol{P}_{\boldsymbol{K}} \\ -\boldsymbol{P}_{\boldsymbol{K}}\boldsymbol{B}_2\boldsymbol{R}^{-1}\boldsymbol{B}_2^{\rm T}\boldsymbol{P}_{\boldsymbol{K}} + \boldsymbol{I}_2 = \boldsymbol{0}, \end{aligned} \tag{11}$$

where $\boldsymbol{B}_1 = [1, 0]^{\rm T}$, $\boldsymbol{B}_2 = [0, 1]^{\rm T}$, and $R > 0$.

Let

$$\begin{aligned} \boldsymbol{\phi}_F(t) &= [\boldsymbol{\phi}_1^{\rm T}(t), \boldsymbol{\phi}_2^{\rm T}(t), \ldots, \boldsymbol{\phi}_{N-1}^{\rm T}(t)]^{\rm T}, \\ \hat{\boldsymbol{\phi}}_F(t) &= [\hat{\boldsymbol{\phi}}_1^{\rm T}(t), \hat{\boldsymbol{\phi}}_2^{\rm T}(t), \ldots, \hat{\boldsymbol{\phi}}_{N-1}^{\rm T}(t)]^{\rm T}, \\ \widetilde{\boldsymbol{\phi}}_F(t) &= \boldsymbol{\phi}_F(t) - \hat{\boldsymbol{\phi}}_F(t), \\ \overline{\boldsymbol{\eta}}_3(t) &= [\eta_{13}(t), \eta_{23}(t), \ldots, \eta_{(N-1)3}(t)]^{\rm T}. \end{aligned}$$

Under protocol (10), the multi-agent system formed by Eqs. (1) and (2) can be written as

$$\begin{cases} \dot{\boldsymbol{\phi}}_F(t) = \big(\boldsymbol{I}_{N-1} \otimes \big(\boldsymbol{B}_1\boldsymbol{B}_2^{\rm T} + \boldsymbol{B}_2\boldsymbol{\alpha}\big) \\ \quad +\boldsymbol{L}_1 \otimes \boldsymbol{B}_2\boldsymbol{K}\big)\,\boldsymbol{\phi}_F(t) + (\boldsymbol{L}_2 \otimes \boldsymbol{B}_2\boldsymbol{K})\boldsymbol{\phi}_N(t) \\ \quad - (\boldsymbol{L}_1 \otimes \boldsymbol{B}_2\boldsymbol{K} - \boldsymbol{I}_{N-1} \otimes \boldsymbol{B}_2\boldsymbol{\alpha})\,\boldsymbol{h}_F(t) \\ \quad +(\boldsymbol{I}_{N-1} \otimes \boldsymbol{B}_2\boldsymbol{B}_2^{\rm T})\dot{\boldsymbol{h}}_F(t) + \overline{\boldsymbol{\eta}}_3(t) \otimes \boldsymbol{B}_2 \\ \quad - \big(\boldsymbol{I}_{N-1} \otimes \big(\boldsymbol{B}_1\boldsymbol{B}_2^{\rm T} + \boldsymbol{B}_2\boldsymbol{\alpha}\big) \\ \quad + \boldsymbol{L}_1 \otimes \boldsymbol{B}_2\boldsymbol{K}\big)\,\widetilde{\boldsymbol{\phi}}_F(t), \\ \dot{\boldsymbol{\phi}}_N(t) = \big(\boldsymbol{B}_1\boldsymbol{B}_2^{\rm T} + \boldsymbol{B}_2\boldsymbol{\alpha}\big)\,\boldsymbol{\phi}_N(t). \end{cases} \tag{12}$$

What is more, similar to Freidovich and Khalil (2008), Jiang et al. (2015), and Ran et al. (2017b), the control injected into the system is bounded by $M_i{\rm sat}(u_i(t)/M_i)$, where M_i is the saturation bound, and ${\rm sat}(\cdot)$ is the saturation function defined by ${\rm sat}(\nu) = {\rm sign}(\nu)\cdot\min\{1, |\nu|\}$.

3.2 Time-varying formation tracking protocol analysis

Let $\boldsymbol{U}_F \in \mathbb{R}^{(N-1)\times(N-1)}$ be a nonsingular matrix such that $\boldsymbol{U}_F^{-1}\boldsymbol{L}_1\boldsymbol{U}_F = \boldsymbol{J}_F$, where $\boldsymbol{J}_F$ is the Jordan canonical form of $\boldsymbol{L}_1$. Define $\boldsymbol{\theta}_i(t) = \boldsymbol{\phi}_i(t) - \boldsymbol{h}_i(t)$, $i \in F$, $\boldsymbol{\theta}_F(t) = [\boldsymbol{\theta}_1^{\rm T}(t), \boldsymbol{\theta}_2^{\rm T}(t), \ldots, \boldsymbol{\theta}_{N-1}^{\rm T}(t)]^{\rm T}$, and

$$\boldsymbol{\varsigma}(t) = (\boldsymbol{U}_F^{-1} \otimes \boldsymbol{I}_2)\boldsymbol{\theta}_F(t) - (\boldsymbol{U}_F^{-1}\boldsymbol{1}_{N-1} \otimes \boldsymbol{I}_2)\boldsymbol{\phi}_N(t). \tag{13}$$

Then, the following lemma holds:

Lemma 2 The multi-agent system formed by Eqs. (1) and (2) achieves time-varying formation tracking under protocol (10) if and only if

$$\lim_{t\to\infty} \boldsymbol{\varsigma}(t) = \boldsymbol{0}_{(2N-2)\times 1}. \tag{14}$$

Proof Let $\boldsymbol{T} = \begin{bmatrix} \boldsymbol{U}_F & \boldsymbol{1}_{N-1} \\ \boldsymbol{0}_{(N-1)\times 1} & 1 \end{bmatrix}$, and consequently $\boldsymbol{T}^{-1} = \begin{bmatrix} \boldsymbol{U}_F^{-1} & -\boldsymbol{U}_F^{-1}\boldsymbol{1}_{N-1} \\ \boldsymbol{0}_{(N-1)\times 1} & 1 \end{bmatrix}$. By Lemma 1, we obtain $-\boldsymbol{L}_1^{-1}\boldsymbol{L}_2 = \boldsymbol{1}_{N-1}$, which implies that

$$\boldsymbol{L}_1\boldsymbol{1}_{N-1} + \boldsymbol{L}_2 = \boldsymbol{0}_{(N-1)\times 1}. \tag{15}$$

From Eq. (15), we can obtain

$$\boldsymbol{T}^{-1}\boldsymbol{L}\boldsymbol{T} = \begin{bmatrix} \boldsymbol{J}_F & \boldsymbol{0} \\ \boldsymbol{0} & \boldsymbol{0} \end{bmatrix}. \tag{16}$$

Define $\boldsymbol{\phi}(t) = [\boldsymbol{\phi}_F^{\rm T}(t), \boldsymbol{\phi}_N^{\rm T}(t)]^{\rm T}$ and $\boldsymbol{\vartheta}(t) = \boldsymbol{\phi}(t) - [\boldsymbol{I}_2, \boldsymbol{0}_{2\times 2(N-1)}]^{\rm T}\boldsymbol{h}_F(t)$. From Eq. (12), we can obtain

$$\begin{aligned}
&\dot{\boldsymbol{\vartheta}}(t)= \\
&\begin{bmatrix} \boldsymbol{I}_{N-1}\otimes\left(\boldsymbol{B}_1\boldsymbol{B}_2^{\mathrm{T}}+\boldsymbol{B}_2\boldsymbol{\alpha}\right) & \mathbf{0} \\ \mathbf{0} & \boldsymbol{B}_1\boldsymbol{B}_2^{\mathrm{T}}+\boldsymbol{B}_2\boldsymbol{\alpha} \end{bmatrix}\boldsymbol{\vartheta}(t) \\
&+(\boldsymbol{L}\otimes\boldsymbol{B}_2\boldsymbol{K})\boldsymbol{\vartheta}(t)-\begin{bmatrix} \boldsymbol{I}_{N-1}\otimes\boldsymbol{B}_1\boldsymbol{B}_2^{\mathrm{T}} \\ \mathbf{0} \end{bmatrix}\boldsymbol{h}_F(t) \\
&+\begin{bmatrix} \boldsymbol{I}_{N-1}\otimes\left(\boldsymbol{B}_1\boldsymbol{B}_2^{\mathrm{T}}+\boldsymbol{B}_2\boldsymbol{\alpha}\right)+\boldsymbol{L}_1\otimes\boldsymbol{B}_2\boldsymbol{K} & \mathbf{0} \\ \mathbf{0} & \mathbf{0} \end{bmatrix} \\
&\cdot\begin{bmatrix} \widetilde{\boldsymbol{\phi}}_F(t) \\ \mathbf{0} \end{bmatrix}-\begin{bmatrix} \boldsymbol{I}_{N-1}\otimes\boldsymbol{B}_1\boldsymbol{B}_1^{\mathrm{T}} \\ \mathbf{0} \end{bmatrix}\dot{\boldsymbol{h}}_F(t) \\
&+\begin{bmatrix} \overline{\boldsymbol{\eta}}_3(t)\otimes\boldsymbol{B}_2 \\ \mathbf{0} \end{bmatrix}. \qquad (17)
\end{aligned}$$

Define $\overline{\boldsymbol{\vartheta}}(t)=[\boldsymbol{\varsigma}^{\mathrm{T}}(t),\boldsymbol{\phi}_N^{\mathrm{T}}(t)]^{\mathrm{T}}$. Then, we obtain

$$\left(\boldsymbol{T}^{-1}\otimes\boldsymbol{I}_2\right)\boldsymbol{\vartheta}(t)=\overline{\boldsymbol{\vartheta}}(t), \qquad (18)$$

and consequently from Eq. (17), the dynamics of $\boldsymbol{\varsigma}(t)$ can be written as

$$\begin{aligned}
\dot{\boldsymbol{\varsigma}}(t)=&\left(\boldsymbol{I}_{N-1}\otimes(\boldsymbol{B}_1\boldsymbol{B}_2^{\mathrm{T}}+\boldsymbol{B}_2\boldsymbol{\alpha})+\boldsymbol{J}_F\otimes\boldsymbol{B}_2\boldsymbol{K}\right)\boldsymbol{\varsigma}(t) \\
&+\left(\boldsymbol{U}_F^{-1}\otimes(\boldsymbol{B}_1\boldsymbol{B}_2^{\mathrm{T}})\right)\boldsymbol{h}_F(t)-\left(\boldsymbol{U}_F^{-1}\otimes(\boldsymbol{B}_1\boldsymbol{B}_1^{\mathrm{T}})\right) \\
&\cdot\dot{\boldsymbol{h}}_F(t)+\left(\boldsymbol{U}_F^{-1}\otimes\left(\boldsymbol{B}_1\boldsymbol{B}_2^{\mathrm{T}}+\boldsymbol{B}_2\boldsymbol{\alpha}\right)\right. \\
&\left.+\boldsymbol{U}_F^{-1}\boldsymbol{L}_1\otimes\boldsymbol{B}_2\boldsymbol{K}\right)\widetilde{\boldsymbol{\phi}}_F(t)+\boldsymbol{U}_F^{-1}\overline{\boldsymbol{\eta}}_3(t)\otimes\boldsymbol{B}_2 \\
=&\left(\boldsymbol{I}_{N-1}\otimes(\boldsymbol{B}_1\boldsymbol{B}_2^{\mathrm{T}}+\boldsymbol{B}_2\boldsymbol{\alpha})+\boldsymbol{J}_F\otimes\boldsymbol{B}_2\boldsymbol{K}\right)\boldsymbol{\varsigma}(t) \\
&+\left(\boldsymbol{U}_F^{-1}\otimes\left(\boldsymbol{B}_1\boldsymbol{B}_2^{\mathrm{T}}+\boldsymbol{B}_2\boldsymbol{\alpha}\right)+\boldsymbol{U}_F^{-1}\boldsymbol{L}_1\otimes\boldsymbol{B}_2\boldsymbol{K}\right) \\
&\cdot\widetilde{\boldsymbol{\phi}}_F(t)+\boldsymbol{U}_F^{-1}\overline{\boldsymbol{\eta}}_3(t)\otimes\boldsymbol{B}_2. \qquad (19)
\end{aligned}$$

Let

$$\boldsymbol{\vartheta}_f(t)=(\boldsymbol{T}\otimes\boldsymbol{I}_2)\left[\mathbf{0}_{1\times 2(N-1)},\boldsymbol{\phi}_N^{\mathrm{T}}(t)\right]^{\mathrm{T}}, \qquad (20)$$

$$\boldsymbol{\vartheta}_{\overline{f}}(t)=(\boldsymbol{T}\otimes\boldsymbol{I}_2)\left[\boldsymbol{\varsigma}^{\mathrm{T}}(t),\mathbf{0}_{1\times 2}\right]^{\mathrm{T}}. \qquad (21)$$

Note that $[\mathbf{0}_{1\times 2(N-1)},\boldsymbol{\phi}_N^{\mathrm{T}}]^{\mathrm{T}}=\boldsymbol{e}_N\otimes\boldsymbol{\phi}_N(t)$, where $\boldsymbol{e}_N\in\mathbb{R}^N$ with 1 as its N^{th} entry and 0 elsewhere. It follows from Eq. (20) that

$$\boldsymbol{\vartheta}_f(t)=\boldsymbol{T}\boldsymbol{e}_N\otimes\boldsymbol{\phi}_N(t)=\mathbf{1}_N\otimes\boldsymbol{\phi}_N(t). \qquad (22)$$

It follows from Eqs. (18), (20), and (22) that

$$\boldsymbol{\vartheta}(t)=\boldsymbol{\vartheta}_f(t)+\boldsymbol{\vartheta}_{\overline{f}}(t), \qquad (23)$$

and $\boldsymbol{\vartheta}_f(t)$ and $\boldsymbol{\vartheta}_{\overline{f}}(t)$ are linearly independent as $\boldsymbol{T}\otimes\boldsymbol{I}_2$ is nonsingular. From Eqs. (22) and (23), one has

$$\boldsymbol{\vartheta}_{\overline{f}}(t)=\boldsymbol{\phi}(t)-\begin{bmatrix} \boldsymbol{I} \\ \mathbf{0}_{2\times 2(N-1)} \end{bmatrix}\boldsymbol{h}_F(t)-\mathbf{1}_N\otimes\boldsymbol{\phi}_N(t), \qquad (24)$$

which is equal to

$$\boldsymbol{\vartheta}_{\overline{f}}(t)=\begin{bmatrix} \boldsymbol{\phi}_F(t)-\boldsymbol{h}_F(t)-\mathbf{1}_N\otimes\boldsymbol{\phi}_N(t) \\ \mathbf{0}_{2\times 2(N-1)} \end{bmatrix}. \qquad (25)$$

From Eq. (25), it holds that the multi-agent system formed by Eqs. (1) and (2) achieves time-varying formation tracking under protocol (10) if and only if

$$\lim_{t\to\infty}\boldsymbol{\vartheta}_{\overline{f}}(t)=\mathbf{0}_{2N\times 1}. \qquad (26)$$

Since $\boldsymbol{T}\otimes\boldsymbol{I}_2$ is nonsingular, it then follows from Eq. (22) that condition (26) is satisfied if and only if Eq. (14) is satisfied. The proof of Lemma 2 is completed.

Remark 4 Note that the result stated in Lemma 2 is generalized from Dong et al. (2017a,b), in which the followers are modeled by linear time-invariant second-order dynamics and the velocity vector of each follower is available for control design. However, we should point out that this generalization is not straightforward, because of the more complex agent dynamics and the coupling of the ESO. It can be clearly observed from the dynamics of $\boldsymbol{\vartheta}(t)$ and $\boldsymbol{\varsigma}(t)$ specified by Eqs. (17) and (19), respectively.

To proceed, select the Lyapunov function candidate

$$V_{\boldsymbol{\varsigma}}(\boldsymbol{\varsigma}(t))=\boldsymbol{\varsigma}^{\mathrm{T}}(t)(\boldsymbol{I}_{N-1}\otimes\boldsymbol{P}_{\boldsymbol{K}})\boldsymbol{\varsigma}(t). \qquad (27)$$

Let

$$\begin{aligned}
\tau=&\sup_{\boldsymbol{\varsigma}(t)\in\mathbb{R}^{2N-2},\|\boldsymbol{\varsigma}(t)\|\le\|\boldsymbol{\varsigma}(0)\|}V_{\boldsymbol{\varsigma}}(\boldsymbol{\varsigma}(t))+1, \\
\varOmega_0=&\{\boldsymbol{\varsigma}(t)\in\mathbb{R}^{2N-2}|V_{\boldsymbol{\varsigma}}(\boldsymbol{\varsigma}(t))\le\tau\}, \\
\varOmega_1=&\{\boldsymbol{\varsigma}(t)\in\mathbb{R}^{2N-2}|V_{\boldsymbol{\varsigma}}(\boldsymbol{\varsigma}(t))\le\tau+1\}.
\end{aligned}$$

Lemma 3 Consider the closed-loop system formed by Eqs. (1), (2), (6), and (10). Assume that the saturation bounds M_i, $i\in F$, are appropriately selected and Assumptions 1–3 are satisfied. Then there exists $\varepsilon_0>0$ such that for all $\varepsilon\in(0,\varepsilon_0)$ and any initial conditions of the closed-loop system, $\boldsymbol{\varsigma}(t)\in\varOmega_1$, $\forall t\in[0,\infty)$.

Proof (For notation simplicity, a time-varying vector $\boldsymbol{\rho}(t)$ will be replaced by $\boldsymbol{\rho}$ in the proof of Lemma 3) We prove Lemma 3 by contradiction. Suppose Lemma 3 is false. Considering $\boldsymbol{\varsigma}$ is continuous with respect to t, $\boldsymbol{\varsigma}(0)\in\varOmega_0-\partial\varOmega_0$, and $\boldsymbol{u}_i$ is bounded, there exist t_1, t_2, and ε-independent t_0 such that $t_2>t_1>t_0>0$ and

$$\begin{cases} V_{\boldsymbol{\varsigma}}(\boldsymbol{\varsigma}(t_1))=\tau, \\ \tau+1<V_{\boldsymbol{\varsigma}}(\boldsymbol{\varsigma}(t_2))\le\tau+2, \\ \tau<V_{\boldsymbol{\varsigma}}(\boldsymbol{\varsigma}(t))\le\tau+1,\ t\in(t_1,t_2). \end{cases} \qquad (28)$$

The differentiation of the extended state ξ_i, $i \in F$, can be computed as

$$\begin{aligned}\dot{\xi}_i =& \dot{x}_i \frac{\partial f_i}{\partial x_i}(x_i, v_i) + \dot{v}_i \frac{\partial f_i}{\partial v_i}(x_i, v_i) + \dot{d}_i \\ =& v_i \frac{\partial f_i}{\partial x_i}(x_i, v_i) + \dot{d}_i \\ &+ \left(f_i(x_i, v_i) + d_i + M_i \mathrm{sat}\left(\frac{u_i}{M_i}\right)\right) \frac{\partial f_i}{\partial v_i}(x_i, v_i).\end{aligned} \tag{29}$$

Considering Eq. (28) and Assumption 1, we can conclude that there exists ε-independent positive constants N_i, $i \in F$, such that $|\dot{\xi}_i| \le N_i$, $\forall t \in [0, t_2]$.

Note that the matrix $\boldsymbol{E}$ specified by Eq. (7) is Hurwitz, and there exists a positive definite matrix $\boldsymbol{P_E}$ that satisfies $\boldsymbol{P_E E} + \boldsymbol{E}^{\mathrm{T}} \boldsymbol{P_E} = -\boldsymbol{I}_3$. Define the Lyapunov function candidate $V_i(\boldsymbol{\eta}_i) = \boldsymbol{\eta}_i^{\mathrm{T}} \boldsymbol{P_E} \boldsymbol{\eta}_i$, $i \in F$, and let $\lambda_{i1} = \lambda_{\min}(\boldsymbol{P_E})$ and $\lambda_{i2} = \lambda_{\max}(\boldsymbol{P_E})$. It follows that

$$\begin{aligned}&\lambda_{i1} \|\boldsymbol{\eta}_i\|^2 \le V_i(\boldsymbol{\eta}_i) \le \lambda_{i2} \|\boldsymbol{\eta}_i\|^2, \\ &\left|\frac{\partial V_i}{\partial \eta_{i3}}(\boldsymbol{\eta}_i)\right| \le 2\lambda_{i2} \|\boldsymbol{\eta}_i\|.\end{aligned} \tag{30}$$

Then computing the time derivative of $V_i(\boldsymbol{\eta}_i)$ in the interval $[0, t_2]$, in view of Eq. (9) and inequality (30), yields

$$\begin{aligned}\frac{\mathrm{d}V_i}{\mathrm{d}t}(\boldsymbol{\eta}_i) =& \frac{1}{\varepsilon}\left(\sum_{j=1}^{2} \left(\eta_{i(j+1)} - l_j \eta_{i1}\right) \frac{\partial V_i}{\partial \eta_{ij}}(\boldsymbol{\eta}_i)\right. \\ &\left. - l_3 \eta_{i1} \frac{\partial V_i}{\partial \eta_{i3}}(\boldsymbol{\eta}_i)\right) + \dot{\xi}_i \frac{\partial V_i}{\partial \eta_{i3}}(\boldsymbol{\eta}_i) \\ \le& -\frac{1}{\varepsilon}\|\boldsymbol{\eta}_i\|^2 + 2\lambda_{i2} N_i \|\boldsymbol{\eta}_i\| \\ \le& -\frac{1}{\lambda_{i2}\varepsilon} V_i(\boldsymbol{\eta}_i) + 2\lambda_{i2} N_i \frac{\sqrt{V_i(\boldsymbol{\eta}_i)}}{\sqrt{\lambda_{i1}}}.\end{aligned} \tag{31}$$

Let $\boldsymbol{\eta} = [\boldsymbol{\eta}_1^{\mathrm{T}}, \boldsymbol{\eta}_2^{\mathrm{T}}, \ldots, \boldsymbol{\eta}_{N-1}^{\mathrm{T}}]^{\mathrm{T}}$ and

$$V_{\boldsymbol{\eta}}(\boldsymbol{\eta}) = \sum_{i=1}^{N-1} V_i(\boldsymbol{\eta}_i). \tag{32}$$

By inequality (31), the time derivative of $V_{\boldsymbol{\eta}}(\boldsymbol{\eta})$ in the interval $[0, t_2]$ satisfies

$$\begin{aligned}\frac{\mathrm{d}V_{\boldsymbol{\eta}}}{\mathrm{d}t}(\boldsymbol{\eta}) =& \sum_{i=1}^{N-1} \frac{\mathrm{d}V_i}{\mathrm{d}t}(\boldsymbol{\eta}_i) \\ \le& \sum_{i=1}^{N-1} \left(-\frac{1}{\lambda_{i2}\varepsilon} V_i(\boldsymbol{\eta}_i) + 2\lambda_{i2} N_i \frac{\sqrt{V_i(\boldsymbol{\eta}_i)}}{\sqrt{\lambda_{i1}}}\right) \\ \le& -\frac{1}{\varepsilon} \varPi_1 V_{\boldsymbol{\eta}}(\boldsymbol{\eta}) + \varPi_2 \sqrt{V_{\boldsymbol{\eta}}(\boldsymbol{\eta})},\end{aligned} \tag{33}$$

where

$$\varPi_1 = \min_{i \in F}\left\{\frac{1}{\lambda_{i2}}\right\}, \ \varPi_2 = \max_{i \in F}\left\{\frac{2\sqrt{N-1}\lambda_{i2} N_i}{\sqrt{\lambda_{i1}}}\right\}.$$

Considering $\frac{\mathrm{d}V_{\boldsymbol{\eta}}}{\mathrm{d}t}(\boldsymbol{\eta}) = 2\sqrt{V_{\boldsymbol{\eta}}(\boldsymbol{\eta})} \frac{\mathrm{d}\sqrt{V_{\boldsymbol{\eta}}(\boldsymbol{\eta})}}{\mathrm{d}t}$, inequality (33) can be rewritten as

$$\frac{\mathrm{d}\sqrt{V_{\boldsymbol{\eta}}(\boldsymbol{\eta})}}{\mathrm{d}t} \le -\frac{1}{2\varepsilon} \varPi_1 \sqrt{V_{\boldsymbol{\eta}}(\boldsymbol{\eta})} + \frac{\varPi_2}{2}. \tag{34}$$

It follows from inequality (34) that $\forall t \in [0, t_2]$,

$$\begin{aligned}\sqrt{V_{\boldsymbol{\eta}}(\boldsymbol{\eta})} \le& \left(\sqrt{V_{\boldsymbol{\eta}}(\boldsymbol{\eta}(0))} - \frac{\varPi_2}{\varPi_1}\varepsilon\right) \mathrm{e}^{-\frac{\varPi_1}{2\varepsilon}t} + \frac{\varPi_2}{\varPi_1}\varepsilon \\ \le& \left(\sqrt{\sum_{i=1}^{N-1} \lambda_{i2} \|\boldsymbol{\eta}_i(0)\|^2} - \frac{\varPi_2}{\varPi_1}\varepsilon\right) \mathrm{e}^{-\frac{\varPi_1}{2\varepsilon}t} \\ &+ \frac{\varPi_2}{\varPi_1}\varepsilon.\end{aligned} \tag{35}$$

Since $\|\boldsymbol{\eta}_i(0)\|^2 = \frac{1}{\varepsilon^4}|x_i(0) - \hat{x}_i(0)|^2 + \frac{1}{\varepsilon^2}|v_i(0) - \hat{v}_i(0)|^2 + |\xi_i(0) - \hat{\xi}_i(0)|^2 = O\left(\frac{1}{\varepsilon^4}\right)$, $i \in F$, it can be concluded that the right-hand side of inequality (35) converges to 0 as $\varepsilon \to 0$ in the time interval $[t_0, t_2]$. It follows from inequality (30) that $\|\boldsymbol{\eta}_i\| \to 0$ as $\varepsilon \to 0$ in the time interval $[t_0, t_2]$. Note that $|\hat{x}_i| \le |x_i| + \varepsilon^2 |\eta_{i1}|$, $|\hat{v}_i| \le |v_i| + \varepsilon |\eta_{i2}|$, $|\hat{\xi}_i| \le |\xi_i| + |\eta_{i3}|$, $i \in F$. Together with inequality (28), and Assumptions 1 and 3, it enables one to select appropriate M_i, $i \in F$, such that the control is out of saturation in the time interval $[t_0, t_2]$. That is $M_i \mathrm{sat}(u_i(t)/M) = u_i(t)$, $i \in F$, $\forall t \in [t_0, t_2]$.

By Eq. (19), the time derivative of $V_{\boldsymbol{\varsigma}}(\boldsymbol{\varsigma})$ in the time interval $[t_0, t_2]$ can be computed as

$$\begin{aligned}\frac{\mathrm{d}V_{\boldsymbol{\varsigma}}}{\mathrm{d}t}(\boldsymbol{\varsigma}) =& \dot{\boldsymbol{\varsigma}}^{\mathrm{T}}(\boldsymbol{I} \otimes \boldsymbol{P_K})\boldsymbol{\varsigma} + \boldsymbol{\varsigma}^{\mathrm{T}}(\boldsymbol{I} \otimes \boldsymbol{P_K})\dot{\boldsymbol{\varsigma}} \\ =& \boldsymbol{\varsigma}^{\mathrm{T}}\left(\boldsymbol{I}_{N-1} \otimes (\boldsymbol{B}_1 \boldsymbol{B}_2^{\mathrm{T}} + \boldsymbol{B}_2 \boldsymbol{\alpha}) + \boldsymbol{J}_F \otimes \boldsymbol{B}_2 \boldsymbol{K}\right)^{\mathrm{T}} \\ &\cdot (\boldsymbol{I} \otimes \boldsymbol{P_K})\boldsymbol{\varsigma} + \widetilde{\boldsymbol{\phi}}_F^{\mathrm{T}}\left(\boldsymbol{U}_F^{-1} \otimes (\boldsymbol{B}_1 \boldsymbol{B}_2^{\mathrm{T}} + \boldsymbol{B}_2 \boldsymbol{\alpha})\right. \\ &\left. + \boldsymbol{U}_F^{-1} \boldsymbol{L}_1 \otimes \boldsymbol{B}_2 \boldsymbol{K}\right)^{\mathrm{T}} (\boldsymbol{I} \otimes \boldsymbol{P_K})\boldsymbol{\varsigma} \\ &+ \left(\boldsymbol{U}_F^{-1} \overline{\boldsymbol{\eta}}_3 \otimes \boldsymbol{B}_2\right)^{\mathrm{T}} (\boldsymbol{I} \otimes \boldsymbol{P_K})\boldsymbol{\varsigma} \\ &+ \boldsymbol{\varsigma}^{\mathrm{T}}(\boldsymbol{I} \otimes \boldsymbol{P_K})\left(\boldsymbol{I}_{N-1} \otimes (\boldsymbol{B}_1 \boldsymbol{B}_2^{\mathrm{T}} + \boldsymbol{B}_2 \boldsymbol{\alpha})\right. \\ &\left. + \boldsymbol{J}_F \otimes \boldsymbol{B}_2 \boldsymbol{K}\right)\boldsymbol{\varsigma} + \boldsymbol{\varsigma}^{\mathrm{T}}(\boldsymbol{I} \otimes \boldsymbol{P_K}) \\ &\cdot \left(\boldsymbol{U}_F^{-1} \otimes (\boldsymbol{B}_1 \boldsymbol{B}_2^{\mathrm{T}} + \boldsymbol{B}_2 \boldsymbol{\alpha}) + \boldsymbol{U}_F^{-1} \boldsymbol{L}_1 \otimes \boldsymbol{B}_2 \boldsymbol{K}\right) \widetilde{\boldsymbol{\phi}}_F \\ &+ \boldsymbol{\varsigma}^{\mathrm{T}}(\boldsymbol{I} \otimes \boldsymbol{P_K})\left(\boldsymbol{U}_F^{-1} \overline{\boldsymbol{\eta}}_3 \otimes \boldsymbol{B}_2\right).\end{aligned} \tag{36}$$

From Eq. (11), the matrix $\boldsymbol{\varPhi} = \boldsymbol{\varPsi} + \boldsymbol{\varPsi}^{\mathrm{T}}$, where $\boldsymbol{\varPsi} = \left(\boldsymbol{I}_{N-1} \otimes (\boldsymbol{B}_1 \boldsymbol{B}_2^{\mathrm{T}} + \boldsymbol{B}_2 \boldsymbol{\alpha}) + \boldsymbol{J}_F \otimes \boldsymbol{B}_2 K\right)^{\mathrm{T}} (\boldsymbol{I} \otimes \boldsymbol{P_K})$, is negative definite. Let $\kappa = \lambda_{\max}(\boldsymbol{\Phi}) < 0$. It follows from Eq. (36) that $\forall t \in [t_0, t_2]$,

$$\frac{\mathrm{d}V_{\varsigma}}{\mathrm{d}t}(\boldsymbol{\varsigma}) \le \kappa\|\boldsymbol{\varsigma}\|^2 + N_0\|\boldsymbol{\varsigma}\|\|\boldsymbol{\eta}\|, \tag{37}$$

where N_0 is an ε-independent positive constant. Since $\forall t \in [t_1, t_2]$, $\tau \le V_{\varsigma}(\boldsymbol{\varsigma})) \le \tau + 2$, and $\|\boldsymbol{\eta}\| \to 0$ as $\varepsilon \to 0$, there exists ε_0 such that for any $\varepsilon \in (0, \varepsilon_0)$,

$$\frac{\mathrm{d}V_{\varsigma}}{\mathrm{d}t}(\boldsymbol{\varsigma}) < 0, \ \forall t \in [t_1, t_2], \tag{38}$$

which contradicts inequality (28). Thus, there exists $\varepsilon_0 > 0$ such that for any $\varepsilon \in (0, \varepsilon_0)$ and any initial condition of the closed-loop system, $\boldsymbol{\varsigma} \in \Omega_1$, $\forall t \in [0, \infty)$. This completes the proof of Lemma 3.

Theorem 1 Consider the closed-loop system formed by Eqs. (1), (2), (6), and (10). Assume that the saturation bounds M_i, $i \in F$, are appropriately selected and that Assumptions 1–3 are satisfied. For any initial condition of the closed-loop system and $T > 0$,

$$\lim_{\varepsilon \to 0} \|\boldsymbol{\eta}_i(t)\| = 0, \ i \in F, \tag{39}$$

uniformly in $t \in [T, \infty)$, and

$$\lim_{\varepsilon \to 0, t \to \infty} (\boldsymbol{\phi}_i(t) - \boldsymbol{h}_i(t) - \boldsymbol{\phi}_N(t)) = \mathbf{0}_{2\times 1}, \ i \in F. \tag{40}$$

Proof From Lemma 3, $\boldsymbol{\varsigma}(t) \in \Omega_1$ for all $\varepsilon \in (0, \varepsilon_0)$ and $t \in [0, \infty)$, it follows that inequality (35) holds for $t \in [0, \infty)$. From inequality (35), we can obtain that for any $T > 0$, $\|\boldsymbol{\eta}_i(t)\| \to 0$, $i \in F$, uniformly in the time interval $[T, \infty)$, as $\varepsilon \to 0$. Consequently, from inequality (37), we have $\boldsymbol{\varsigma}(t) \to 0$ as $\varepsilon \to 0$ and $t \to \infty$. Finally, from Lemma 2, we can conclude that Eq. (40) holds. The proof of Theorem 1 is completed.

Remark 5 It should be pointed out that the ESO estimation errors and the time-varying formation tracking errors can be specified in the sense that there exists $t_0 > 0$ such that

$$\begin{aligned} \sup\nolimits_{t \in [t_0, \infty)} |x_i(t) - \hat{x}_i(t)| &= O(\varepsilon^3), \\ \sup\nolimits_{t \in [t_0, \infty)} |v_i(t) - \hat{v}_i(t)| &= O(\varepsilon^2), \\ \sup\nolimits_{t \in [t_0, \infty)} |\xi_i(t) - \hat{\xi}_i(t)| &= O(\varepsilon), \\ \lim\nolimits_{t \to \infty} \sup \|\boldsymbol{\phi}_i(t) - \boldsymbol{h}_i(t) - \boldsymbol{\phi}_N(t)\| &= O(\varepsilon), i \in F. \end{aligned}$$

Theoretically, to achieve better estimation and tracking performance, we can select the value of ε to be arbitrarily small. However, there will be some limitations on the value of ε due to both noises and sampling constraints when the protocol is implemented on computers (Jiang et al., 2015; Ran et al., 2017b). What is more, similar to Freidovich and Khalil (2008) and Ran et al. (2017b), it is generally not straightforward to calculate the saturation bounds M_i, $i \in F$. In practice, the values of ε and M_i, $i \in F$, can be selected by a simple trial-and-error procedure, based on the obtained estimation and formation tracking performance. Our simulation experience and many examples in the literature, e.g., Freidovich and Khalil (2008) and Ran et al. (2017b), indicate that it is very easy to select a group of satisfactory ε and M_i, $i \in F$.

Remark 6 In the case that the position and velocity vectors of the followers are both available for control design, the following reduced-order ESO can be designed:

$$\begin{cases} \dot{\hat{v}}_i(t) = \hat{\xi}_i(t) + \frac{l_1}{\varepsilon}(v_i(t) - \hat{v}_i(t)) + u_i(t), \\ \dot{\hat{\xi}}_i(t) = \frac{l_2}{\varepsilon^2}(v_i(t) - \hat{v}_i(t)), \end{cases} \tag{41}$$

where $[l_1, l_2] \in \mathbb{R}^2$ is selected such that the matrix $\begin{bmatrix} -l_1 & 1 \\ -l_2 & 0 \end{bmatrix}$ is Hurwitz. Correspondingly, the time-varying formation tracking protocol (10) is replaced by

$$\begin{aligned} &u_i(t) = \\ &\boldsymbol{K} \sum_{j \in N_i, j \ne N} a_{ij} \left((\boldsymbol{\phi}_i(t) - \boldsymbol{h}_i(t)) - (\boldsymbol{\phi}_j(t) - \boldsymbol{h}_j(t))\right) \\ &+ \boldsymbol{K} a_{iN} \left((\boldsymbol{\phi}_i(t) - \boldsymbol{h}_i(t)) - \boldsymbol{\phi}_N(t)\right) \\ &+ \boldsymbol{\alpha} \left(\boldsymbol{\phi}_i(t) - \boldsymbol{h}_i(t)\right) + \dot{h}_{iv}(t) - \hat{\xi}_i(t), \ i \in F. \end{aligned} \tag{42}$$

Redefine $\boldsymbol{\eta}_i(t) = [\eta_{i1}(t), \eta_{i2}(t)]^{\mathrm{T}}$, $i \in F$, with $\eta_{i1}(t) = \frac{1}{\varepsilon}(v_i(t) - \hat{v}_i(t))$ and $\eta_{i2}(t) = \xi_i(t) - \hat{\xi}_i(t)$. It can be readily verified that the results stated in Theorem 1 hold under protocol (42).

4 Application to target enclosing of multiple UAVs

In this section, we apply the theoretical approach to deal with the target enclosing problem for a group of UAVs, and compare it with existing approaches.

The formation control design of UAVs falls into a two-loop structure: the outer loop guides a UAV toward the specified position with a specified velocity, and yields the attitude commands, while the inner-loop tracks the attitude commands. Due to the inherent spectral separation between the two loops, the outer-loop and inner-loop can be designed separately (Wang and Xin, 2013). The design of the outer-loop is our focus in this study.

Using the feedback linearization approach, the outer-loop dynamics of a UAV can be approximately described by a double integrator (Wang et al., 2007; Wang and Xin, 2013; Dong et al., 2015; Liao et al., 2017) or a second-order linear time-invariant system (Dong et al., 2017a,b). However, it is now well recognized that the feedback linearization method lacks robust capability if the nonlinearity is uncertain (Isidori, 1989). In fact, the nonlinear dynamics of a UAV are generally uncertain due to the uncertainties in the mass, the moments of inertia, and so on. What is more, the outer-loop dynamics of a UAV may be disturbed by external disturbance, such as wind. Thus, it is important and meaningful to consider the formation problem for UAVs subject to unknown nonlinear dynamics and external disturbance.

Consider a multi-UAV system with five followers and one leader in the horizontal $X-Y$ plane; that is, $n=2$. Fig. 1 shows the interaction topology of the multi-UAV system. Different from Wang et al. (2007), Wang and Xin (2013), Dong et al. (2015, 2017a,b), and Liao et al. (2017), the dynamics of each following UAV are described by the second-order uncertain nonlinear system (1), with position $\boldsymbol{x}_i(t)=[x_{iX}(t),x_{iY}(t)]^{\mathrm{T}}$ and velocity $\boldsymbol{v}_i(t)=[v_{iX}(t),v_{iY}(t)]^{\mathrm{T}}$. Assume $\alpha_{\boldsymbol{x}}=-0.64$ and $\alpha_{\boldsymbol{v}}=0$. The five following UAVs are required to maintain a time-varying circular formation while surrounding the moving target in the horizontal $X-Y$ plane. Specifically, the time-varying formation for the following UAVs is given as

$$\boldsymbol{h}_i(t)=\begin{bmatrix}20\cos(0.5t+2(i-1)\pi/5)\\-10\sin(0.5t+2(i-1)\pi/5)\\20\sin(0.5t+2(i-1)\pi/5)\\10\cos(0.5t+2(i-1)\pi/5)\end{bmatrix},$$
$$i=1,2,3,4,5.$$

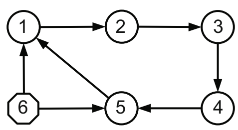

Fig. 1 Network topology

From $\boldsymbol{h}_F(t)$, it can be verified that when the desired formation tracking is achieved, the states of the five followers will keep a time-varying circular pentagon while enclosing the moving target.

4.1 Effectiveness verification

To verify the effectiveness of the proposed approach, let $f_i(\boldsymbol{x}_i(t),\boldsymbol{v}_i(t))=$
$$\begin{bmatrix}\frac{1}{2}x_{iX}(t)\sin(x_{iY}(t))+\frac{1}{3}x_{iY}(t)\sin(x_{iX}(t))\\\frac{1}{3}v_{iX}(t)\sin(v_{iY}(t))+\frac{1}{2}v_{iY}(t)\sin(v_{iX}(t))\end{bmatrix},$$
$$d_i(t)=\frac{5}{i}\sin(t),\ i=1,2,3,4,5.$$
Select $\delta=1$. Solving the Riccati equation (11) with $\boldsymbol{R}=\boldsymbol{I}_2$, one obtains $\boldsymbol{K}=\boldsymbol{I}_2\otimes[-1.8340,-4.8501]$. The ESO (6) is designed with observer gain $[3,3,1]^{\mathrm{T}}$ and $\varepsilon=0.01$. Saturation bounds are selected as $M_i=50$, $i=1,2,3,4,5$. The initial conditions of the UAVs are set as $x_{iX}(0)=\hbar$, $x_{iY}(0)=\hbar$, $v_{iX}(0)=\hbar$, and $v_{iY}(0)=\hbar$, $i=1,2,3,4,5$, where $\hbar$ is a random distribution value on the interval $(0,1)$; $x_{6X}(0)=5$, $x_{6Y}(0)=5$, $v_{6X}(0)=2$, and $v_{6Y}(0)=2$. The initial conditions of the ESOs are all set as null.

Fig. 2 shows the state trajectories of the six UAVs within 10 s, where the final states of the followers and the leader are marked by hexagrams and circle, respectively. It can be observed that the states of the five followers form a circular pentagon formation, and the state of the leader stays in the center of the pentagon. Fig. 3 illustrates the position and velocity trajectory snapshots of the six UAVs at $t=10$ s, $t=14$ s, and $t=18$ s. One can see that both the position and velocity components of the five following UAVs form the time-varying circular pentagon formation, which keeps rotating around the leader UAV. Fig. 4 depicts the states and the ESO estimated states corresponding to follower 1, from which one can see that the states $\boldsymbol{x}_1(t)$, $\boldsymbol{v}_1(t)$, and the extended state $\boldsymbol{\xi}_1(t)$ are well estimated by the ESO.

4.2 Comparison with previous work

To further show the superiority of the proposed approach, we compare the proposed approach with the approach in Dong et al. (2017a,b). Suppose that the five following UAVs are modeled by the following second-order time-invariant linear system subject to

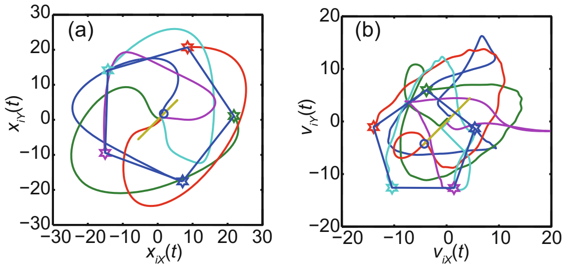

Fig. 2 Position (a) and velocity (b) trajectories within t=10 s

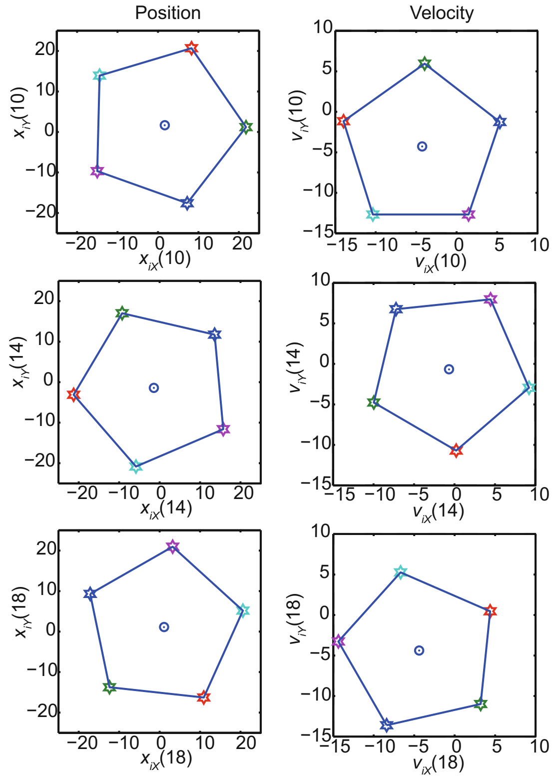

Fig. 3 Position and velocity trajectory snapshots of the six UAVs at t=10 s, t=14 s, and t=18 s

external disturbance:

$$\begin{cases} \dot{\boldsymbol{x}}_i(t) = \boldsymbol{v}_i(t), \\ \dot{\boldsymbol{v}}_i(t) = \alpha_{\boldsymbol{x}}\boldsymbol{x}_i(t) + \alpha_{\boldsymbol{v}}\boldsymbol{v}_i(t) + d_i(t) + u_i(t), \\ \boldsymbol{y}_i(t) = \boldsymbol{x}_i(t), \ i = 1,2,3,4,5. \end{cases} \tag{43}$$

In Dong et al. (2017a,b), the following time-varying formation tracking protocol is proposed:

$$\begin{aligned} u_i(t) = & \\ \boldsymbol{K} & \sum_{j\in N_i, j\neq N} a_{ij}\left((\boldsymbol{\phi}_i(t) - \boldsymbol{h}_i(t)) - (\boldsymbol{\phi}_j(t) - \boldsymbol{h}_j(t))\right) \\ & + \boldsymbol{K}a_{iN}\left((\boldsymbol{\phi}_i(t) - \boldsymbol{h}_i(t)) - \boldsymbol{\phi}_N(t)\right) \\ & - \boldsymbol{\alpha}\boldsymbol{h}_i(t) + \dot{h}_{iv}(t), \ i = 1,2,3,4,5. \end{aligned} \tag{44}$$

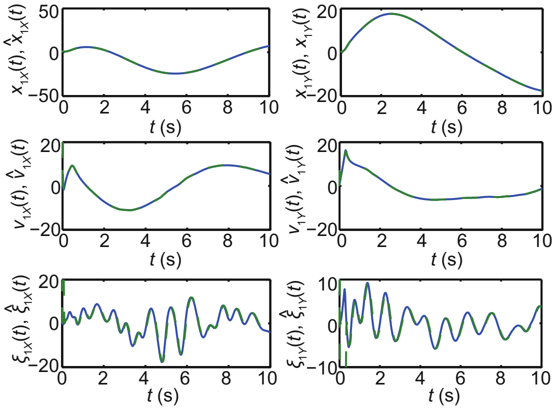

Fig. 4 States (solid lines) and ESO estimated states (dashed lines) of follower 1

Note that protocol (44) is based on full state-feedback and that the influence of external disturbance is not taken into account. Let $d_i(t) = 25\sin(t)$, i = 1, 2, 3, 4, 5. To make a fair comparison, all the parameters and initial conditions are the same as before. Figs. 5 and 6 depict the simulation results under protocols (44) and (10), respectively. Fig. 5 shows that the time-varying formation tracking failed. However, Fig. 6 shows that the desired time-varying formation tracking was achieved satisfactorily by the proposed protocol. The main reason

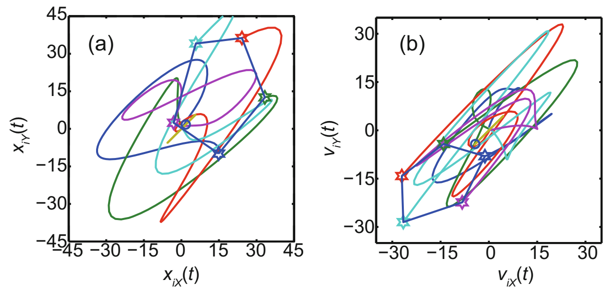

Fig. 5 Position (a) and velocity (b) trajectories within t=10 s under protocol (44)

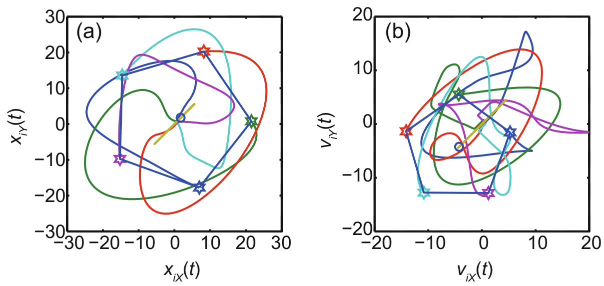

Fig. 6 Position (a) and velocity (b) trajectories within t=10 s under protocol (10)

is that in the proposed protocol, the external disturbance is estimated by the ESO, and compensated for in the control protocol in real time. From this viewpoint, the proposed approach provides a more practical solution to the time-varying formation tracking problem.

5 Conclusions and future work

In this study, we study the time-varying formation tracking problem for uncertain second-order nonlinear multi-agent systems, and propose an ESO based time-varying formation tracking protocol. The proposed approach provides a novel and practical solution to the time-varying formation tracking problem for multi-agent systems, especially in the case where the agent is subject to unknown nonlinear dynamics and external disturbance. An application to the target enclosing of UAVs shows the effectiveness and superiority of the proposed approach. Extension of the proposed approach to more complex formation problems, such as the formation-containment problem (Chen LM et al., 2017; Li et al., 2018), is part of our future work. What is more, note that the proposed protocol relies on the knowledge of λ_1. In Li et al. (2015), a consensus protocol was proposed which was independent of any global information of the communication graph. Designing a fully distributed time-varying formation tracking protocol based on the idea proposed in Li et al. (2015) is under investigation.

References

Bechlioulis CP, Rovithakis GA, 2017. Decentralized robust synchronization of unknown high order nonlinear multi-agent systems with prescribed transient and steady state performance. *IEEE Trans Autom Contr*, 62(1):123-134. https://doi.org/10.1109/TAC.2016.2535102

Castañeda LA, Luviano-Juárez A, Chairez I, 2015. Robust trajectory tracking of a delta robot through adaptive active disturbance rejection control. *IEEE Trans Contr Syst Technol*, 23(4):1387-1398. https://doi.org/10.1109/TCST.2014.2367313

Chang XY, Li YL, Zhang WY, et al., 2015. Active disturbance rejection control for a flywheel energy storage system. *IEEE Trans Ind Electron*, 62(2):991-1001. https://doi.org/10.1109/TIE.2014.2336607

Chen LM, Li CJ, Mei J, et al., 2017. Adaptive cooperative formation-containment control for networked Euler-Lagrange systems without using relative velocity information. *IET Contr Theory Appl*, 11(9):1450-1458. https://doi.org/10.1049/iet-cta.2016.1185

Chen YY, Wang ZZ, Zhang Y, et al., 2017a. A geometric extension design for spherical formation tracking control of second-order agents in unknown spatiotemporal flowfields. *Nonl Dynam*, 88(2):1173-1186. https://doi.org/10.1007/s11071-016-3303-2

Chen YY, Zhang Y, Wang ZZ, 2017b. An adaptive backstepping design for formation tracking motion in an unknown Eulerian specification flowfield. *J Franklin Inst*, 354(14):6217-6233. https://doi.org/10.1016/j.jfranklin.2017.07.020

Cui RX, Ge SS, How BVE, et al., 2010. Leader-follower formation control of underactuated autonomous underwater vehicles. *Ocean Eng*, 37(17-18):1491-1502. https://doi.org/10.1016/j.oceaneng.2010.07.006

Dong XW, Yu BC, Shi ZY, et al., 2015. Time-varying formation control for unmanned aerial vehicles: theories and applications. *IEEE Trans Contr Syst Technol*, 23(1):340-348. https://doi.org/10.1109/TCST.2014.2314460

Dong XW, Xiang J, Han L, et al., 2017a. Distributed time-varying formation tracking analysis and design for second-order multi-agent systems. *J Intell Robot Syst*, 86(2):277-289. https://doi.org/10.1007/s10846-016-0421-5

Dong XW, Zhou Y, Ren Z, et al., 2017b. Time-varying formation tracking for second-order multi-agent systems subjected to switching topologies with application to quadrotor formation flying. *IEEE Trans Ind Electron*, 64(6):5014-5024. https://doi.org/10.1109/TIE.2016.2593656

Du HB, Cheng MZQ, Wen GH, 2016. Leader-following attitude consensus for spacecraft formation with rigid and flexible spacecraft. *J Guid Contr Dynam*, 39(4):944-951. https://doi.org/10.2514/1.G001273

Freidovich LB, Khalil HK, 2008. Performance recovery of feedback-linearization-based designs. *IEEE Trans Autom Contr*, 53(10):2324-2334. https://doi.org/10.1109/TAC.2008.2006821

Galzi D, Shtessel Y, 2006. UAV formations control using high order sliding modes. American Control Conf, p.4249-4254. https://doi.org/10.1109/ACC.2006.1657386

Guo BZ, Zhao ZL, 2011. On the convergence of an extended state observer for nonlinear systems with uncertainty. *Syst Contr Lett*, 60(6):420-430. https://doi.org/10.1016/j.sysconle.2011.03.008

Guo J, Yan GF, Lin ZY, 2010. Local control strategy for moving-target-enclosing under dynamically changing network topology. *Syst Contr Lett*, 59(10):654-661. https://doi.org/10.1016/j.sysconle.2010.07.010

Han JQ, 2009. From PID to active disturbance rejection control. *IEEE Trans Ind Electron*, 56(3):900-906. https://doi.org/10.1109/TIE.2008.2011621

Herbst G, 2016. Practical active disturbance rejection control: bumpless transfer, rate limitation, and incremental algorithm. *IEEE Trans Ind Electron*, 63(3):1754-1762. https://doi.org/10.1109/TIE.2015.2499168

Hu WH, Camacho EF, Xie LH, 2018. Output feedback control based on state and disturbance estimation. https://arxiv.org/abs/1801.06058

Isidori A, 1989. Nonlinear Control Systems. Springer-Verlag Berlin Heidelberg. https://doi.org/10.1007/978-3-662-02581-9

Jiang TT, Huang CD, Guo L, 2015. Control of uncertain nonlinear systems based on observers and estimators. *Automatica*, 59:35-47. https://doi.org/10.1016/j.automatica.2015.06.012

Khalil HK, 2002. Nonlinear Systems (3rd Ed.). Prentice Hall, New Jersey, USA.

Leonard NE, Paley DA, Davis RE, et al., 2010. Coordinated control of an underwater glider fleet in an adaptive ocean sampling field experiment in Monterey Bay. *J Field Robot*, 27(6):718-740. https://doi.org/10.1002/rob.20366

Li CJ, Chen LM, Guo YN, et al., 2018. Formation-containment control for networked Euler-Lagrange systems with input saturation. *Nonl Dynam*, 91(2):1307-1320. https://doi.org/10.1007/s11071-017-3946-7

Li SB, Zhang J, Li XL, et al., 2017. Formation control of heterogeneous discrete-time nonlinear multi-agent systems with uncertainties. *IEEE Trans Ind Electron*, 64(6):4730-4740. https://doi.org/10.1109/TIE.2017.2674590

Li XX, Xie LH, 2018. Dynamic formation control over directed networks using graphical Laplacian approach. *IEEE Trans Autom Contr*, 63(11):3761-3774. https://doi.org/10.1109/TAC.2018.2798808

Li ZK, Wen GH, Duan ZS, et al., 2015. Designing fully distributed consensus protocols for linear multi-agent systems with directed graphs. *IEEE Trans Autom Contr*, 60(4):1152-1157. https://doi.org/10.1109/TAC.2014.2350391

Liao F, Teo R, Wang JL, et al., 2017. Distributed formation and reconfiguration control of VTOL UAVs. *IEEE Trans Contr Syst Technol*, 25(1):270-277. https://doi.org/10.1109/TCST.2016.2547952

Lin ZY, Ding W, Yan GF, et al., 2013. Leader-follower formation via complex Laplacian. *Automatica*, 49(6):1900-1906. https://doi.org/10.1016/j.automatica.2013.02.055

Liu Y, Jia YM, 2012. An iterative learning approach to formation control of multi-agent systems. *Syst Contr Lett*, 61(1):148-154. https://doi.org/10.1016/j.sysconle.2011.10.011

Lotfi N, Zomorodi H, Landers RG, 2016. Active disturbance rejection control for voltage stabilization in open-cathode fuel cells through temperature regulation. *Contr Eng Pract*, 56:92-100. https://doi.org/10.1016/j.conengprac.2016.08.006

Lü J, Chen F, Chen GR, 2016. Nonsmooth leader-following formation control of nonidentical multi-agent systems with directed communication topologies. *Automatica*, 64:112-120. https://doi.org/10.1016/j.automatica.2015.11.004

Meng DY, Jia YM, Du JP, et al., 2014. On iterative learning algorithms for the formation control of nonlinear multi-agent systems. *Automaitca*, 50(1):291-295. https://doi.org/10.1016/j.automatica.2013.11.009

Meng ZY, Ren W, You Z, 2010. Distributed finite-time attitude containment control for multiple rigid bodies. *Automatica*, 46(12):2092-2099. https://doi.org/10.1016/j.automatica.2010.09.005

Oh KK, Ahn HS, 2014. Formation control and network localization via orientation alignment. *IEEE Trans Autom Contr*, 59(2):540-545. https://doi.org/10.1109/TAC.2013.2272972

Oh KK, Park MC, Ahn HS, 2015. A survey of multi-agent formation control. *Automatica*, 53:424-440. https://doi.org/10.1016/j.automatica.2014.10.022

Peng ZH, Wang D, Chen ZY, et al., 2013. Adaptive dynamic surface control for formations of autonomous surface vehicles with uncertain dynamics. *IEEE Trans Contr Syst Technol*, 21(2):513-520. https://doi.org/10.1109/TCST.2011.2181513

Ran MP, Wang Q, Dong CY, et al., 2017a. Backstepping active disturbance rejection control: a delayed activation approach. *IET Contr Theory Appl*, 11(14):2336-2342. https://doi.org/10.1049/iet-cta.2016.1533

Ran MP, Wang Q, Dong CY, 2017b. Active disturbance rejection control for uncertain nonaffine-in-control nonlinear systems. *IEEE Trans Autom Contr*, 62(11):5830-5836. https://doi.org/10.1109/TAC.2016.2641980

Ren W, 2007. Consensus strategies for cooperative control of vehicle formations. *IET Contr Theory Appl*, 1(2):505-512. https://doi.org/10.1049/iet-cta:20050401

Ren W, Sorensen N, 2008. Distributed coordination architecture for multi-robot formation control. *Robot Auton Syst*, 56(4):324-333. https://doi.org/10.1016/j.robot.2007.08.005

Wang JN, Xin M, 2013. Integrated optimal formation control of multiple unmanned aerial vehicles. *IEEE Trans Contr Syst Technol*, 21(5):1731-1744. https://doi.org/10.1109/TCST.2012.2218815

Wang Q, Ran MP, Dong CY, 2016. Robust partial integrated guidance and control for missiles via extended state observer. *ISA Trans*, 65:27-36. https://doi.org/10.1016/j.isatra.2016.08.017

Wang XH, Yadav V, Balakrishnan SN, 2007. Cooperative UAV formation flying with obstacle/collision avoidance. *IEEE Trans Contr Syst Technol*, 15(4):672-679. https://doi.org/10.1109/TCST.2007.899191

Yang AL, Naeem W, Irwin GW, et al., 2014. Stability analysis and implementation of a decentralized formation control strategy for unmanned vehicles. *IEEE Trans Contr Syst Technol*, 22(2):706-720. https://doi.org/10.1109/TCST.2013.2259168

Zhang HW, Lewis FL, 2012. Adaptive cooperative tracking control of higher-order nonlinear systems with unknown dynamics. *Automatica*, 48(7):1432-1439. https://doi.org/10.1016/j.automatica.2012.05.008

Zheng Q, Gao LQ, Gao ZQ, 2012. On validation of extended state observer through analysis and experimentation. *J Dynam Syst Meas Contr*, 134(2):024505. https://doi.org/10.1115/1.4005364

Zhu B, Zaini AHB, Xie LH, 2017. Distributed guidance for interception by using multiple rotary-wing unmanned aerial vehicles. *IEEE Trans Ind Electron*, 64(7):5648-5656. https://doi.org/10.1109/TIE.2017.2677313